

Direct Photons in e^+e^- Annihilation*

E. Laermann[†]
Institut für Theoretische Physik
Technische Hochschule Aachen
D-5100 Aachen, Germany

T. F. Walsh
Deutsches Elektronen-Synchrotron
D-2000 Hamburg-52, Germany

I. Schmitt[‡] and P. M. Zerwas[§]
Stanford Linear Accelerator Center
Stanford University, Stanford, California 94305

(Submitted to Nuclear Physics B)

*Work supported in part by the Department of Energy, contract DE-AC03-76SF00515, and the W. German Bundesministerium für Forschung and Technologie.

[†]Present address: Physics Department, Harvard University, Cambridge, MA.

[‡]Kade Foundation Fellow, on leave from Universität Wuppertal, Wuppertal, Germany.

[§]Kade Foundation Fellow, on leave from Technische Hochschule Aachen, Aachen, Germany.

ABSTRACT

We study the production of direct photons in e^+e^- annihilation

$$e^+e^- \rightarrow \gamma + \text{hadrons}$$

where the high energy photon is emitted at a large angle to a hadron jet or is a fragment of the jet itself. We give the angle and energy dependence of the cross section for photons radiated from the final state quarks, the initial state leptons, and also the interference term.

Large angle radiation by the quarks is only mildly affected by QCD corrections to the parton model. For photons radiated within or near a jet axis, however, the gluon radiative corrections can be large.

We study the phenomenological implications of these corrections at present and future energies. Direct photon production affords a unique view into the short and long distance processes of jet formation. It can help clarify the space-time transition between perturbative and non-perturbative processes in jet development.

1. Introduction

It has long been recognized that direct photon production at large angles can be used to explore the properties and interactions of quarks and gluons at short distances[1,2]. This is because the photons, once produced, leave the short distance regime without further interactions. They allow a direct view of the physics at short distances, where quark and gluon interactions can be treated perturbatively. (By contrast, quarks and gluons themselves have strong interactions when their separations become larger than about 1 fermi and the physics is not yet well understood[3,4].) An especially interesting direct photon reaction is[5,6]

$$e^+ e^- \rightarrow \gamma + \text{hadrons} \quad (1)$$

where the photon is radiated off the final state quarks (fig. 1).

Depending on the transverse momenta between the photon and a quark jet, two different mechanisms give rise to photon radiation.

(a) If the photon is radiated at large angle to the jet (fig. 2a), the lifetime of the quark before radiation is of order $1/Q$. The photon is radiated at a very short distance from the primary interaction which created a quark and antiquark pair. At such short distances, QCD interactions are effectively switched off, and the parton model should apply — at least to a good approximation[5-8]. (Thus this process can be used to measure quark charges.) Gluon radiation and vertex corrections will change the parton model results to order α_s , which is roughly $1/\log(Q)$. While these corrections are asymptotically small, precise measurements can check these nontrivial QCD contributions without having to worry about such things as jet fragmentation. A similar example is the radiative decay of a heavy quark-antiquark state to a photon plus QCD quanta.

(b) If the photon is radiated within a small cone around the quark direction (fig. 2b), $k_{\perp}^2 \lesssim \delta^2 Q^2 \ll Q^2$, there is enough time available for the quark to radiate a number of gluons before the photon is emitted. Under appropriate conditions, the distances involved can still be small enough so that the gluon radiation can be treated perturbatively. Suppose that we require that the quark travel less than a distance of order the inverse QCD scale parameter, Λ^{-1} . Then perturbation theory should be good. This corresponds to quarks of invariant mass $p^2 > \Lambda Q$ or photon emission angles

$$1 \gg \delta \gtrsim \sqrt{\Lambda/Q} \quad (2)$$

Asymptotically, this covers the complete angular range. At finite Q , however, there is a remaining range of quark invariant mass or emission angle

$$\delta \lesssim \mathcal{O}(\sqrt{\Lambda/Q}) \sim \mathcal{O}(10-15^\circ) \quad (3)$$

where the long range — and therefore nonperturbative — interactions of QCD can play a role. It is not possible a priori to say whether or not perturbation theory can be applied in the range (3). Most authors assume that it will work down to parton virtual masses of order a GeV or so, which includes the range (3) at present and future energies. This low parton mass or small photon angle region is, of course, where one would more naturally attempt to describe the radiation by using a model, such as the vector meson dominance model (fig. 2c). It would then seem that the small angle or small transverse momentum photons will be concentrated at very small momenta, as are the hadrons. The precise relation of this type of model to our estimate (3) is not entirely clear. We will return to this question later in the paper. For the present, we will consider

the development of a perturbative shower of partons without specifying where it stops in parton invariant mass or angle. Because of the gluon radiation, photons are radiated with a softer spectrum than expected in Born approximation without gluon emission,

$$D_q^Y(z, Q^2)_{\text{BORN}} \simeq \frac{\alpha}{2\pi} e_q^2 \frac{1 + (1-z)^2}{z} \log \frac{Q^2}{\Lambda^2} . \quad (4)$$

There is a corresponding increase at small values of $z = E/E(\text{beam})$. This is all in the leading logarithm approximation[9-11]. Corrections to this approximation turn out to be important[12] and give further significant decrease of the photon flux at not too large z . This trend is already clear in the leading log calculation, and in the large angle QCD corrections to the Born approximation. The effect is much more pronounced here in the timelike region than in the spacelike regime of deep inelastic electron-photon scattering[9]. Despite this, we of course still expect a fundamental difference between photon and hadron spectra. Hadron spectra decrease rapidly, apparently vanishing as z nears 1. The photon spectra are much harder, being large for large z . In addition, the photon spectrum increases as $\log Q$ while the hadron spectra decrease with Q at large z .

Besides radiation from the quarks, we also expect photons from the electrons or positrons. This is a background process and can be subtracted if the charges in the final state are averaged over. Charge asymmetry measurements at low energies ($Q < 40$ GeV) can exploit the interference of radiation from quarks and leptons to provide yet another check of fractional quark charges[6].

There are, of course, some experimental problems with such measurements. The fractional direct photon rate will be of order of the fine

structure constant, or about one percent of all hadronic events. One will need a lot of hadronic events to do an analysis of this channel. Another problem is the background from neutral pions. At high momentum, both decay photons will merge and fake direct photon events. However, the neutral pion spectrum should fall off rapidly in momentum both transverse to and along the jet axis. There is a large kinematic region where QCD predicts a substantial ratio of direct photons to neutral pions. The background should be manageable there[10]. Moreover, we expect the neutral pion rate to be the average of the rates for positive and negative pions except at low z , where weak decays will lead to a breaking of isospin symmetry. This allows a subtraction of neutral pion spectra at high momentum where confusion with single photons is possible.

Potential difficulties with photon radiation from the electron and positron beams can be expected when the angle between the beams and the observed direct photon becomes small and when the energy of this photon gets very close to the beam energy. Then the rates will become large and the signal from photon radiation by quarks will be swamped. It will probably be necessary to stay away from small photon angles and photon energies very close to $E(\text{beam})$. We are, of course, interested in direct photon distributions relative to the jet axes, and radiation from the beams is uncorrelated with the jet axes. For this reason, we think that the simplest way to analyze data is to exclude the kinematically bad regions we have mentioned, and to plot data as a function of z of the photon and either the angle to the global axis of the hadrons in the event or the transverse momentum of the photon relative to this axis. Measurement of charge asymmetries will not require this of course.

In the next section we rederive the Born cross section via a helicity method. This nicely separates kinematic and dynamical effects for the radiation off quarks, leptons and also the interference term. These expressions are somewhat simpler and easier to understand than the familiar ones. The second part of this section is on the first order QCD corrections to the Born approximation. We adopt the usual angular criterion for defining a QCD jet[14]. This has been applied to the calculations of first order QCD corrections to 3 jet production in the continuum[15]. These corrections turn out to be controllable, though not negligible.

The third section goes into the photon distribution inside a jet or, equivalently, the fragmentation function of a quark to a photon. We consider both the presently accessible energies as well as the next generation of colliders. They will run at the Z boson resonance, which is a convenient way to get a large event rate for direct photons.

2. Hard Photons at Large Angle

As we have remarked, photon radiation from quarks can be treated perturbatively provided the gamma-quark invariant mass is large enough or the emission angle is large. Photon radiation from the electron or positron line can also be treated perturbatively provided the invariant mass of the hadron system is large enough. It can, of course, be dealt with exactly once the cross section for electron positron collisions is known. (It will also be necessary to use information on the topology of the events, since no detector has perfect acceptance.) This assumes that the hadron charges are summed over so that interferences between even and odd charge conjugation amplitudes vanish.

Wide angle bremsstrahlung is interesting for two reasons. First, final states with charge $2/3$ quarks are weighted four times as heavily as those with charge $-1/3$ quarks. This thus involves a different combination of electromagnetic (and weak) charges than does the simple annihilation cross section. This can help to separate out different quark charges — on the Z boson resonance, for example, where quarks with different charges are otherwise produced with nearly the same rates. The second source of interest in this process is due to the close relation to three jet events, with the photon substituting for the gluon in that case. It will be instructive to compare the higher order QCD corrections to the photon rate and spectrum with those for gluon radiation.

Using a now standard notation for 3 quantum final states, we parameterize the photon in fig. 3 by its fractional energy z and the polar angle ϑ . We average over the azimuthal angle around the beams so as to eliminate the effect of transverse beam polarization.* The quark and antiquark are characterized by their energies and the azimuthal angle χ between the $(e^+e^-\gamma)$ and the $(q\bar{q}\gamma)$ planes. The angles ϑ_q and $\vartheta_{\bar{q}}$ between quark, antiquark and photon are fixed by the energies, $\cos\vartheta_q = 1 + 2(1-x_q-z)/x_q z$ as is the transverse momentum, $x_{\perp} = 2[(1-z)(1-x_q)(1-x_{\bar{q}})]^{1/2}/z$. All energies are, of course, measured in units of the beam energy. The same variables can be used to describe the final state if QCD corrections are taken into account if one redefines the parton jets as Sterman-Weinberg jets.

* Longitudinal beam polarization is discussed in the first appendix. For some transverse beam polarization effects see ref. 8.

A. Cross Sections in Born Approximation

The cross section for photon radiation from massless quarks in lowest order in the strong coupling is, from the first diagram of fig. 4a and in units of the electromagnetic μ pair cross section,

$$\frac{1}{\sigma_{\mu\mu}} \frac{d\sigma^q}{dz dx_q d\cos\vartheta d\chi} = \frac{3\alpha}{128 \pi^2} e_q^2 \sum_{hel} R_q(Q^2) \frac{S + h_e h_q A}{(1-x_q)(1-x_{\bar{q}})} \quad (5)$$

The sum runs over all helicities of quark and electron, $h_{e,q} = +1, -1$. Antiparticles carry the opposite helicities to the particles, because of the vector interaction and vanishing quark mass. The function S is built up of transverse and longitudinal virtual photon and Z boson contributions.

$$S = (1 + \cos^2\vartheta) \left[x_q^2 + x_{\bar{q}}^2 - x_{\perp}^2 \right] + 2 \sin^2\vartheta x_{\perp}^2 + \sin^2\vartheta \cos 2\chi x_{\perp}^2 - \sin 2\vartheta \cos\chi x_{\perp} \left[x_q \cos\vartheta_q - x_{\bar{q}} \cos\vartheta_{\bar{q}} \right] \quad (6)$$

The term A involves a forward-backward asymmetry of the photon with respect to the electron direction. This is a consequence of the parity violating Z exchange,

$$A = 2 \cos\vartheta \left[x_q^2 \cos\vartheta_q - x_{\bar{q}}^2 \cos\vartheta_{\bar{q}} \right] - 2 \sin\vartheta \cos\chi x_{\perp} (x_q + x_{\bar{q}}) \quad (7)$$

This term vanishes if the jet charges are summed over. (The corresponding functions for massive quarks can be extracted from ref. 16.)

The coefficient R_q is the usual ratio R, but for fixed initial and final fermion helicities. Defining a "charge"

$$f_q(Q^2) = e_q - \frac{G_F Q^2}{8 \sqrt{2} \pi \alpha} \frac{(v_e - h_e a_e)(v_q - h_q a_q)}{(Q^2 - M_Z^2 + iM_Z \Gamma_Z)/M_Z^2} \quad (8)$$

we have

$$R_q(Q^2) = 3 |f_q(Q^2)|^2 \quad (9)$$

The definition of the vector and axial couplings of the fermions to the Z boson are $v_j = \mp 1 - 4Q_j \sin^2 \vartheta_w$ and $a_j = \mp 1$ where the minus (plus) sign is for negatively (positively) charged particles. At low energies, $Q^2 \ll M_Z^2$, the cross section is just $3 \sum e_q^4$, the sum of the fourth powers of the quark charges. The cross section is singular for very soft or collinear photons. In this kinematic region the Born approximation breaks down, as the emission time scale becomes large, of order the inverse of the quark-photon virtual mass. The formula applies (up to corrections of order the strong coupling) provided a cut is made in the emission angle of the photon, and its energy is kept larger than some minimum fraction of the beam energy.

The cross section for emission from the initial lepton lines (fig. 4b) can be written in terms of the same functions S and A. It is

$$\frac{1}{\sigma_{\mu\mu}} \frac{d\sigma^e}{dz dx_q d\cos\vartheta d\chi} = \frac{3\alpha}{32 \pi^2} \sum_{\text{hel}} R_q(Q'^2) \frac{S + h_e h_q A}{z^2 (1-z) \sin^2 \vartheta} \quad (10)$$

Note that R_q is evaluated here at a $Q'^2 = (1-z)Q^2$. This contribution gets large for soft photons ($z \rightarrow 0$) and for those collinear with the beams. We also remarked earlier on the singularity as $Q' \rightarrow 0$, or when the photon energy $z \rightarrow 1$. It is necessary to keep away from these regions.

The interference of the above two contributions is a bit more complicated. At low energies, it induces charge asymmetries[6]. However, it is also very important in the region of large electroweak interferences, even if the jet charges are not measured. We have

$$\frac{1}{\sigma_{\mu\mu}} \frac{d\sigma^i}{dz dx_q d\cos\vartheta d\chi} = - \frac{3\alpha}{64 \pi^2} e_q \sum_{\text{hel}} \mathcal{R}e \left[R'_q \frac{\tilde{S} + h_e h_q \tilde{A} + i(h_q \tilde{T}_q + h_e \tilde{T}_e)}{z^2 \sin^2 \vartheta} \right] \quad (11)$$

where

$$R'_q = 3f_q(Q^2) f_q^*(Q'^2) \quad (12)$$

and

$$\begin{aligned} \tilde{S} = & (1 + \cos^2 \vartheta) \cos \chi x_{\perp} \kappa_1 \frac{1 + (1-z)^2}{1-z} + 2 \sin^2 \vartheta \left[5 \cos \chi + \cos 3\chi \right] x_{\perp} \\ & + 4 \sin 2\vartheta \cos^2 \chi (x_q - x_{\bar{q}}) \frac{2-z}{z} \end{aligned} \quad (13)$$

$$\tilde{A} = 2 \cos \vartheta \cos \chi x_{\perp} \kappa_2 \frac{1 + (1-z)^2}{1-z} - 8 \sin \vartheta \cos^2 \chi (2-z) \quad (14)$$

The functions \tilde{T}_q and \tilde{T}_e contribute only in the Z region,

$$\tilde{T}_q = (1 + \cos^2 \vartheta) \sin \chi x_{\perp} \kappa_2 \frac{2-z}{1-z} + 2z \sin 2\vartheta \sin 2\chi \quad (15)$$

$$\tilde{T}_e = -2 \cos \vartheta \sin \chi x_{\perp} \kappa_1 \frac{2-z}{1-z} - 4 \sin \vartheta \sin 2\chi (x_q - x_{\bar{q}}) \quad (16)$$

The κ 's are abbreviations of

$$\kappa_{1,2} = \frac{1 - x_q}{1 - x_{\bar{q}}} \pm \frac{1 - x_{\bar{q}}}{1 - x_q} \quad .$$

Notice that this angular dependence is as complicated as is allowed by helicity arguments. There are other representations of this cross section in the literature[6,8]. Despite its complexity the present form is better, as it makes clear the kinematic dependences which follow from angular momentum considerations.

Cross Section Estimates

We will look into the QCD corrections in the next chapter. It is nonetheless interesting and instructive to examine the overall scale of the cross sections, as shown by the Born terms. In fig. 5 we show the Born cross section in $SU(2) \times U(1)$. To keep away from singularities, we chose a cut in the thrust $\max(z, x_q, x_{\bar{q}}) < .975$. The restriction that

the polar angle lie between 45 and 135 degrees is to stay away from the lepton beam. Under these conditions the rate is about 1 percent, as we mentioned earlier. The rise above the Z resonance is due to photon radiation by the leptons, with the final hadron mass equal to the Z mass. This is shown in more detail in fig. 5b. On the Z, almost all the photons are radiated off the quarks. This is a simple way to avoid background from radiation off the beams. Note that the photon yields in hadronic and muonic events are related to each other by

$$\frac{\sum \sigma(q\bar{q}\gamma)}{\sum \sigma(q\bar{q})} = \frac{\sum e_q^2 R_q}{\sum R_q} \frac{\sigma(\mu\bar{\mu}\gamma)}{\sigma(\mu\bar{\mu})} \quad (17)$$

(Remember that we are still using the Born approximation.) The proportionality factor measures the Z couplings to quarks, with up and down quarks weighted differently than in the pure quark-antiquark cross section,

$$\frac{R_u}{R_d} \approx \frac{v_u^2 + a_u^2}{v_d^2 + a_d^2} \approx 0.8 \quad (18a)$$

$$\frac{e_u^2 R_u}{e_d^2 R_d} \approx \frac{e_u^2}{e_d^2} \frac{v_u^2 + a_u^2}{v_d^2 + a_d^2} \approx 3 \quad (18b)$$

(In eq. (18), we took $\sin^2 \theta_w = 0.23$.) Photon radiation breaks the near quark democracy on the Z.

A relation like (17) holds between gluon distributions in 3 jet events and photon distributions,

$$\frac{d\sigma(q\bar{q}G)}{\sigma(q\bar{q})} = \frac{4}{3} \frac{\alpha_s}{\alpha} \frac{d\sigma(\mu\bar{\mu}\gamma)}{\sigma(\mu\bar{\mu})} \quad (19)$$

This affords a nice way to see clearly the close relation of QCD as a field theory of strong interactions and QED, the prototype of all field theories.

In the z range from 0.2 to 0.8 the gamma spectrum is little affected by the thrust cut. Figure 6 shows the spectrum at 30 GeV and on the Z resonance. (In this connection, see also ref. 8.) This shows typical bremsstrahlung behavior, $dN/dz \propto z^{-1}$. It is interesting to look at how the various contributions to the cross section depend on the angle between the photon and the quark jet axis. Figure 7 shows that up to angles of the order of 40 degrees the dominant mechanism is photon radiation by the quarks. This is therefore the most interesting part of phase space for extracting the direct photon signal.

Charge Asymmetries

At low energies the charge asymmetries are of course due to the interference of diagrams where the photon is radiated by the beams and by the quarks. (This leaves the hadrons in a state with $C = -$ and $C = +$, respectively.) At higher energies, charge asymmetries can also arise as a result of C -noninvariant Z exchange. One can either study these asymmetries for jets or for single particle distributions, say $e^+e^- \rightarrow \gamma + \pi^\pm + X$. The former requires the measurement of quark charges. Prescriptions for this purpose have been worked out in the parton model. These charge asymmetries offer a tool for measuring quark charges in a purely electromagnetic process[6]. The ratio of the $\gamma + q\bar{q}$ to $\gamma + \mu\bar{\mu}$ cross section is given by the third power of the quark charges,

$$\frac{d\sigma(\gamma q\bar{q}) - d\sigma(\gamma \bar{q}q)}{d\sigma(\gamma \mu\bar{\mu}) - d\sigma(\gamma \bar{\mu}\mu)} = 3 e_q^3 = \begin{cases} + 8/9 & \text{for up quarks} \\ - 1/9 & \text{for down quarks} \end{cases} \quad (20)$$

The asymmetries predicted for quark jets in the present energy range around 30 GeV are large. Fixing the photon angle at 90 degrees, the difference between the number of $(u+\bar{d})$ and $(\bar{u}+d)$ jets is on the average

of the order of 50 percent. (Note that u and \bar{d} generate the same π^\pm profile.) In fig. 8 we show the asymmetry as a function of the angle between photon and jet. We think that this asymmetry will be experimentally accessible over quite a wide angular range. If we estimate that there is about a 2:1 chance that the fastest particle in a u jet is positively charged, then the asymmetry is still of order 20 percent when measured using the fastest particle in the jet. We would thus expect a measurable asymmetry with of the order 100 inclusive photon events. This means a sample of order 10000 hadronic events in all, which should be an achievable goal.

We might remark from fig. 8 that the asymmetry is small for photons at low transverse momentum to the quark. As a consequence, it is possible to calculate the QCD radiative corrections to the asymmetry.

An extended footnote: Neutral Pion Background. At high photon energy it may prove hard to separate photons from the overlapping showers from neutral pion decay. This presents a potential threat to the direct photon measurement. We have already mentioned using charged pion spectra to subtract this background. We now comment a bit further on this problem.

(a) Large angle single pions arise due to so-called higher twist effects[17]. As the rate of single photon production is governed by α , we might expect this factor to be replaced by

$$\sim \alpha_s^2 f_\pi^2 / p_\perp^2 \sim (10^{-3} - 10^{-4}) / p_\perp^2 \text{ (GeV}^2\text{)}$$

for single pions. (This has also been noticed recently in ref. 18.)

Provided the transverse momentum is greater than about 2 GeV we expect no trouble from this sort of contamination.

(b) Large angle pions will occur in gluon bremsstrahlung events. This sort of background can be eliminated by requiring that no other particles accompany the direct "photon."

B. Higher Order QCD Corrections

Our distributions so far have been calculated with the strong interaction corrections ignored. This is justified to a first approximation by the asymptotic freedom of QCD -- provided, of course, that we restrict ourselves to large angle photon radiation. The next order strong interaction corrections involve gluon bremsstrahlung and vertex corrections (fig. 4). They modify the cross section by terms of order the inverse of $\log(Q)$. The diagrams are similar to those which appear in the radiative corrections to three-jet events. A notable exception is that diagrams involving the 3 gluon vertex are absent. Before we go on to the details of this problem, we would like to add some general comments on the calculation.

The interference between the vertex correction and the Born term is infrared singular (negative infinite). This singularity is cancelled by a positive divergence due to soft gluon radiation. The result is finite once the parameters of the jet resolution are chosen. These parameters might be the opening angle and fractional energy of a jet, or a jet mass. Unfortunately, this picture lacks a convincing motivation in terms of a space-time development of the (nonperturbative!) jet. The problem is quite simple in terms of the jet or parton invariant mass. The cancellation of infrared divergences takes place as the parton invariant mass approaches zero. But from our earlier arguments it is trivial to see that this requires partons to propagate to large distances in space. However,

we know that confinement or nonperturbative effects are dominant at large distances. No parton or group of partons can propagate freely to distances of many fermi. What this means is that the divergences which we compute and formally cancel, are in fact completely wiped out by nonperturbative effects. They do not exist. Because of this we do not think that the higher order corrections in QCD can be looked on as a purely technical problem. There seems to be an underlying physics issue for which no clear solution is yet in sight. The most direct and unambiguous way to proceed is simply to see whether the naive way of cancelling the divergences works or not (or to what extent it works). Direct photon production is useful here, because it affords a view of the "femto-universe" unobscured by the fragmentation effect which would be there if we were to look at jet distributions instead.

There are two resolution parameters used in the literature. One method, popular in QCD Monte Carlo studies, introduces mass cutoffs[19]. Parton pairs whose invariant mass falls below a critical value, $\sqrt{p^2} \lesssim 5$ GeV at present energies, are attributed to one jet. Another method follows the Sterman-Weinberg definition of physical jets by requiring that partons form separate jets only if the energy of the partons is large enough, and the angles between the partons is also large enough[14,15]. To define the photon plus jet final states, we have adopted the Sterman-Weinberg criterion. We calculate the cross section for events where all but a fraction $\epsilon/2$ of the total energy is distributed among two separated jet cones of (full) opening angle δ and the photon. The QCD radiative corrections were calculated for the cross section integrated over the azimuthal angle χ and also summed over jet charges. The bremsstrahlung cross

section' (σ^q) and (σ^e) and the interference term (σ^i) get modified in the following way:

$$\frac{1}{\sigma_{\mu\mu}} \frac{d\sigma^q}{dz dx_q d\cos\vartheta} = \frac{3\alpha}{32\pi} e_q^2 \sum_{hel} R_q(Q^2) \left\{ (1 + \cos^2\vartheta) \left[\frac{x_q^2 + x_{\bar{q}}^2 - x_L^2}{(1-x_q)(1-x_{\bar{q}})} - \frac{4}{3} \frac{\alpha_s}{\pi} s_T^q \right] \right. \\ \left. + 2 \sin^2\vartheta \left[\frac{x_L^2}{(1-x_q)(1-x_{\bar{q}})} - \frac{4}{3} \frac{\alpha_s}{\pi} s_L^q \right] \right\} \quad (21)$$

$$\frac{1}{\sigma_{\mu\mu}} \frac{d\sigma^e}{dz dx_q d\cos\vartheta} = \frac{3\alpha}{8\pi} \sum_{hel} R_q(Q'^2) \left\{ (1 + \cos^2\vartheta) \left[\frac{x_q^2 + x_{\bar{q}}^2 - x_L^2}{z^2(1-z)\sin^2\vartheta} - \frac{4}{3} \frac{\alpha_s}{\pi} s_T^e \right] \right. \\ \left. + 2 \sin^2\vartheta \left[\frac{x_L^2}{z^2(1-z)\sin^2\vartheta} - \frac{4}{3} \frac{\alpha_s}{\pi} s_L^e \right] \right\} \quad (22)$$

$$\frac{1}{\sigma_{\mu\mu}} \frac{d\sigma^i}{dz dx_q d\cos\vartheta} = -\frac{3\alpha}{16\pi} e_q \sum_{hel} h_e h_q \mathcal{R}e \left\{ R_q' \left[-4 \frac{2-z}{x^2} - \frac{4}{3} \frac{\alpha_s}{\pi} s_i \right] \right\} \quad (23)$$

where x_q and $x_{\bar{q}}$ now denote the two jet energies. The functions depend on the jet energies, the opening angle of the jets and the fraction of energy that is lost to straggling low energy quanta. The functions are complicated, and we list those terms which do not vanish as $\epsilon, \delta \rightarrow 0$ in Appendix B.

It may be useful to sketch the derivation of these expressions in the leading log approximation ($\epsilon, \delta \rightarrow 0$). In this case the corrections are universal,

$$d\sigma_{\text{BORN}} \rightarrow d\sigma = d\sigma_{\text{BORN}} \left[1 - \frac{8\alpha_s}{3\pi} \log \epsilon \log \frac{\delta^2}{4} \right] \quad (24)$$

In the equivalent photon (or gluon) approximation, the fraction of events we lose by gluon bremsstrahlung off quarks and antiquarks at angles $\geq \delta/2$ and carrying off energy $\geq \epsilon$ is just[20]

$$\frac{1}{2} \cdot \frac{4}{3} \frac{\alpha_s}{2\pi} \int_{\delta/2} \frac{d\delta'^2}{\delta'^2} \int_{\epsilon} dx \frac{1 + (1-x)^2}{x} \approx \frac{8\alpha_s}{3\pi} \log \epsilon \log \frac{\delta^2}{4} \quad . \quad (25)$$

This loss can be substantial if ϵ and δ are chosen small. Note that also the single logarithms, which cannot be obtained so easily, are universal (cf Appendix B).

We present some numbers in fig. 10, where the change in various parts of the cross section to first order in α_s is shown. The change is generally of order 25% when we choose parameters $\epsilon = 0.2$ and $\delta/2 = 22.5^\circ$. A similar picture emerges for the photon spectra and for the dependence of the cross section on the angle between photon and quark jets, figs. 11 and 12. The ratio of longitudinal to transverse cross sections is almost unaffected by QCD corrections, a consequence of the overwhelming universal log contributions. The same is true for the asymmetry whose α_s -correction is too small to be seen in fig. 8. Note the large increase of the QCD corrections at small angles $\theta_{\gamma q}$ in fig. 12. We will come back to this point in the next section.

3. Quark Fragmentation to a Photon

When the angle between a radiated photon and its parent jet becomes small, the photon is emitted at large times. This means that there is time available for multiple gluon emission before the photon itself is radiated. The momentum of the parent quark is degraded by gluon emission and as a result the photon spectrum is softer than in Born approximation. The photon spectrum is thus a nice indirect measure of the gluon bremsstrahlung by quarks. (There is a small contribution to the photon spectrum from radiation off quark-antiquark pairs generated by gluons. This is not important.) We naturally expect that the photon spectrum from

quarks will be much harder than the spectrum of hadrons in a quark jet[5]. The latter vanishes quite fast as the fractional momentum $z \rightarrow 1$; the photon spectrum remains substantial out to very near $z = 1$. The softening of the photon spectrum by gluon radiation has previously been calculated in the leading logarithm approximation[9-11]. In a second step, extending the cut vertex method[21], it has been shown that the next to leading order contributions substantially affect the moments of the photon spectrum calculated in leading order[12].

Defining the cross section for electron-positron to photon plus hadrons as

$$\frac{1}{\sigma_{\text{had}}} \frac{d\sigma}{dz d \cos\vartheta} = \frac{8}{3} (1 + \cos^2\vartheta) \bar{F}_T(z, Q^2) + \frac{4}{3} \sin^2\vartheta \bar{F}_L(z, Q^2) \quad (26)$$

we show, in fig. 13, the correction to the Born term expression for the transverse and longitudinal part,

$$\bar{F}_T(z, Q^2)_{\text{BORN}} = \frac{1}{\sum_{R_q}} \sum_{R_q} e_q^2 \frac{\alpha}{\pi} \frac{1 + (1-z)^2}{z} \log \frac{Q^2(1-z)}{\Lambda^2} \quad (27a)$$

$$\bar{F}_L(z, Q^2)_{\text{BORN}} = \frac{1}{\sum_{R_q}} \sum_{R_q} e_q^2 \frac{\alpha}{\pi} \cdot 4 \frac{1-z}{z} \quad (27b)$$

due to quark gluon interactions. The corrections are even larger than in the related process of deep inelastic electron-photon scattering[13]. The spectra were obtained from ref. 12 in the MOM scheme with $\Lambda_{\text{MOM}} = 300$ MeV. It has to be kept in mind that these spectra are summed over photons emitted at all angles to the jets. The QCD corrections are, of course, only large for the photons emitted near a jet.

Much of the higher order correction to the photon structure function seems to be of a kinematic origin. Phase space integrals are typically

cut off, at W^2 of order $Q^2(1-z)$, and not just Q^2 . Some of the higher order correction in the inclusive direct photon case may have a similar origin. However, we note that the typical Q^2 in deep inelastic scattering is of order 5 to 10 GeV^2 . In our case it is of order a thousand GeV^2 . Kinematic corrections which appear in a logarithm will naturally be somewhat less important at such large Q^2 .

Taking up again the question of backgrounds, we think that photon radiation by the electron-positron beams is not too important. This should be clear from fig. 7, which shows the dependence on the angle to the jet axis. Since most direct photons are correlated to the jet axis, the background should not be too bad. The contamination by unresolved neutral pion decays is probably more serious, for a similar reason. Photons near a jet axis may be hard to tell from the neutral pions. However, we hope that this can still be achieved at high z by using isospin symmetry to subtract the neutral pion contribution. This should work even if the pions cannot be excluded event-by-event.

In closing, we would like to return to an observation made at the beginning of the paper. We pointed out that there is a substantial angular range $\delta \sim 10-15^\circ$ where the quark which emits the photon has travelled distances exceeding a fermi or so. The question is whether or not one can naively sum up gluon bremsstrahlung diagrams in this kinematic region. Since long distances are involved, the validity of perturbation theory does not seem (to us) to be obviously assured. The question is — what happens in this kinematic range? For very small angles (near the lower limit above), we expect a model such as the vector meson dominance model to work. Photons are emitted at very large distances from the hadrons

generated by the jet formation. Quarks and gluons are not involved directly in this. At the other limit, we expect multiple gluon emission to be the correct physics. Experiments can in principle tell us how the two meld into one another. For simplicity, consider two extreme scenarios.

(a) There is very little perturbative evolution below a parton invariant mass of order 5 GeV or so. (Nonperturbative or confinement effects just swallow partons with mass less than this.) Then we expect that over much of the angular range we mentioned only the radiation by final state hadrons is relevant. However, the momentum or z spectra are then very soft. They vanish rapidly as z nears 1. This would mean that for small angles or photon transverse momenta less than about 2 GeV one would see only a very soft photon spectrum. Above this transverse momentum the spectrum would rapidly become much harder and would be substantial even fairly near $z = 1$. This situation is sketched in fig. 14a.

(b) Perturbative evolution continues down to the virtual parton masses of order the hadron mass -- the rho meson mass, for example. Then over the entire angular range above we expect to see hard photons. (Equivalently, the spectrum remains hard down to transverse momenta of a few hundred MeV.) This situation is sketched in fig. 14b. Only for transverse momenta less than a few hundred MeV do we see very soft photon spectra, falling off fast at large z .

We think that such direct photon experiments, done near the jet axes, can deliver us quite interesting information about the physics of jet formation.

4. Summary

We have discussed direct photon production in electron-positron collisions in some detail, because we think that it is an excellent application of QCD which goes beyond the usual structure function studies. It involves both short and long distances in quite an intriguing way. The study of the space-time development of jets can be done unimpeded by fragmentation of the quantum which is generated inside the "femto-universe." The experiments may have their difficulties, but we believe that the return in the form of new physics understanding may make them well worth it. This would also apply to studies of direct photon production on the Z boson resonance.

Acknowledgements

We benefitted from discussions with S. Brodsky, D. Groom and J. Yelton. Encouragement from A. Böhm, D. Haidt, D. Leith, G. Tarnopolsky, R. Stroynowski and W. Wallraff is gratefully acknowledged. I. Schmitt and P. Zerwas thank S. Drell for the hospitality extended to them in the SLAC theory division, and the Kade Foundation for financial support.

REFERENCES

- [1] H. Fritzsch, M. Gell-Mann and H. Leutwyler, Phys. Lett. B47 (1973) 365; D. J. Gross and F. Wilczek, Phys. Rev. Lett. 30 (1973) 1343; H. D. Politzer, Phys. Rev. Lett. 30 (1973) 1346.
- [2] P. M. Zerwas, Proceedings, 4th Int'l Colloquium on Photon-Photon Interactions, Paris 1981.
- [3] G. Hanson et al., Phys. Rev. Lett. 35 (1975) 1609.
- [4] R. Brandelik et al., Phys. Lett. 86B (1979) 243; D. P. Barber et al., Phys. Rev. Lett. 43 (1979) 830; Ch. Berger et al., Phys. Lett. 86B (1979) 418; W. Bartel et al., Phys. Lett. 91B (1980) 142.
- [5] T. F. Walsh and P. M. Zerwas, Phys. Lett. 44B (1973) 195.
- [6] S. J. Brodsky, C. E. Carlson and R. Suaya, Phys. Rev. D14 (1976) 2264.
- [7] G. Farrer and B. L. Joffe, Phys. Lett. 71B (1977) 118.
- [8] M. Gourdin and F. M. Renard, Nucl. Phys. B162 (1980) 285; F. Delduc et al., Nucl. Phys. B174 (1980) 157.
- [9] C. H. Llewellyn-Smith, Phys. Lett. 79B (1978) 83.
- [10] K. Koller, T. F. Walsh and P. M. Zerwas, Z. Physik C2 (1979) 197.
- [11] W. R. Frazer and J. F. Gunion, Phys. Rev. D20 (1979) 147.
- [12] K. Sasaki, Phys. Rev. D24 (1981) 1177.
- [13] W. Bardeen and A. Buras, Phys. Rev. D20 (1979) 166; D. W. Duke and J. F. Owens, Phys. Rev. D22 (1980) 2280; T. Uematsu and T. F. Walsh, Fermilab PUB-81/55-THY.
- [14] G. Sterman and S. Weinberg, Phys. Rev. Lett. 39 (1977) 1436.
- [15] K. Fabricius, I. Schmitt, G. Kramer and G. Schierholz, DESY 81/35.
- [16] J. Jersák et al., Phys. Rev. D25 (1982) 1218.

- [17] See, e.g., J. F. Gunion, 3rd Int'l Symposium on Elementary Particle Physics, Warsaw, Poland, 1980.
- [18] S. Gupta, Phys. Rev. D24 (1981) 1163; S. L. Grayson and M. P. Tuite, Cambridge Report DAMTP 81/27.
- [19] P. Hoyer et al., Nucl. Phys. B161 (1979) 349; K. Kunszt, Phys. Lett. 99B (1981) 429.
- [20] M. S. Chen and P. M. Zerwas, Phys. Rev. D12 (1975) 187.
- [21] A. H. Mueller, Phys. Rev. D18 (1978) 3705; S. Gupta and A. H. Mueller, Phys. Rev. D20 (1979) 118.

Appendix A

Helicity Cross Sections for $e^+e^- \rightarrow q\bar{q}\gamma$

Since future e^+e^- colliders as the SLC and LEP might be operated with longitudinally polarized beams we shall present in this appendix the photon-production cross section for fixed lepton (and quark) helicities. In contrast to ref. 8, we have calculated the full angular and energy dependence of the cross section; this is necessary when experimental cuts are taken into account. The calculation has been carried out for the Born term as QCD corrections factorize in the leading log approximation. If masses are neglected, the particle and anti-particle helicities are opposite to each other for vector as well as axial-vector couplings of the gauge fields. The notation for energies and angles of the particles is the same as in the second section.

We split the cross section again into a part which is due to bremsstrahlung off quarks (σ^q), bremsstrahlung off leptons (σ^e) and their interference term (σ^i). The helicities of quarks and leptons are characterized by $h_q, h_e = \pm 1$, respectively. Using the generalized charges $f_q(Q^2; h_e, h_q)$ defined in eq. (8), we find the following cross sections (color is summed).

Bremsstrahlung Off Quarks

$$\frac{1}{\sigma_{\mu\mu}} \frac{d\sigma^q(h_e, h_q)}{dz dx_q d\cos\vartheta d\chi} = \frac{9\alpha}{256\pi^2} e_q^2 |f_q(Q^2; h_e, h_q)|^2 L_{mn}(h_e) H_{mn}(h_q)$$

m and n denote the (virtual) γ and Z spin components along the real γ axis; they are summed over. The spin density matrices are given by the following expressions. The lepton tensor is

$$L_{\pm\pm} = 2(\pm\cos\vartheta + h_e)^2$$

$$L_{00} = 4 \sin^2\vartheta$$

$$L_{\pm\mp} = 2 \sin^2\vartheta e^{\pm 2i\chi}$$

$$L_{\pm 0}(\chi) = L_{0\pm}(-\chi) = -2\sqrt{2} \sin\vartheta (\pm\cos\vartheta + h_e) e^{\pm i\chi}$$

and the hadron tensor,

$$H_{\pm\pm} = 2 \left[(x_q^2 + x_{\bar{q}}^2 - x_l^2) \pm h_q (x_q^2 \cos\vartheta_q - x_{\bar{q}}^2 \cos\vartheta_{\bar{q}}) \right] / (1-x_q)(1-x_{\bar{q}})$$

$$H_{00} = 2 H_{\pm\mp} = 4 x_l^2 / (1-x_q)(1-x_{\bar{q}})$$

$$H_{\pm 0} = H_{0\pm} = \sqrt{2} \left[\pm x_l (x_q \cos\vartheta_q - x_{\bar{q}} \cos\vartheta_{\bar{q}}) + h_q x_l (x_q + x_{\bar{q}}) \right] / (1-x_q)(1-x_{\bar{q}})$$

(For transverse lepton polarization, the tensor L_{mn} is changed according to standard rules.) Table 1 shows which electro-weak charge combinations can be measured in photon events under various experimental conditions of beam polarization.

Bremsstrahlung Off Leptons

This part of the cross section can be written in a similar form

$$\frac{1}{\sigma_{\mu\mu}} \frac{d\sigma^e(h_e, h_q)}{dz dx_q d\cos\vartheta d\chi} = \frac{9\alpha}{256 \pi^2} |f_q(Q'^2; h_e, h_q)|^2 \frac{\bar{L}_{mn}(h_e) \bar{H}_{mn}(h_q)}{(1-z)^2}$$

where the lepton tensor is

$$\bar{L}_{\pm\pm} = \frac{4[1 + (1-z)^2]}{z^2 \sin^2\vartheta} (\pm\cos\vartheta + h_e)^2$$

$$\bar{L}_{00} = \frac{16}{z^2} (1-z)$$

$$\bar{L}_{\pm\mp} = \frac{8}{z^2} (1-z) e^{\pm 2i\chi}$$

$$\bar{L}_{\pm 0}(\chi) = \bar{L}_{0\pm}(-\chi) = -4\sqrt{2} \frac{\sqrt{1-z}(2-z)}{z^2 \sin\vartheta} (\pm \cos\vartheta + h_e) e^{\pm i\chi},$$

and the hadron tensor

$$\bar{H}_{\pm\pm} = 2 \left\{ \left[2(1-z) - x_{\perp}^2 \right] \pm h_q x_q x_{\bar{q}} (\cos\vartheta_q - \cos\vartheta_{\bar{q}}) \right\}$$

$$\bar{H}_{00} = 2 \bar{H}_{\pm\mp} = 4 x_{\perp}^2$$

$$\bar{H}_{\pm 0} = \bar{H}_{0\pm} = 2\sqrt{2} x_{\perp} \sqrt{1-z} \left\{ \pm \frac{x_{\bar{q}} - x_q}{z} + h_q \right\}.$$

Interference Term

The interference term is more involved, of course. To keep the notation compact, the sum over the real γ helicities is not carried out (special, simple examples have been discussed in the second section).

$$\frac{1}{\sigma_{\mu\mu}} \frac{d\sigma^i(h_e, h_q)}{dz dx_q d\cos\vartheta d\chi} = -\frac{9\alpha}{256 \pi^2} 2 \operatorname{Re} \left\{ e_q f_q(Q^2; h_e, h_q) f_q^*(Q'^2; h_e, h_q) \right. \\ \left. \cdot \frac{\tilde{L}_{mn}^r(h_e) \tilde{H}_{mn}^r(h_q)}{(1-z)} \right\}$$

The elements of the lepton tensor read, for positive real γ helicity, indicated by the upper index,

$$\tilde{L}_{--}^+ (h_e) = (1-z) \tilde{L}_{++}^+ (-h_e) = \frac{2\sqrt{2}(1-z)}{z \sin\vartheta} (-\cos\vartheta + h_e)^2 e^{-i\chi}$$

$$\tilde{L}_{00}^+ = 4\sqrt{2} \frac{\sqrt{1-z}}{z} \sin\vartheta e^{-i\chi}$$

$$\tilde{L}_{+-}^+ = (1-z) e^{+4i\chi} \tilde{L}_{-+}^+ = 2\sqrt{2} \frac{1-z}{z} \sin\vartheta e^{i\chi}$$

$$\tilde{L}_{0-}^+ (h_e) = -\sqrt{1-z} \tilde{L}_{+0}^+ (-h_e) = -4 \frac{(1-z)}{z} (-\cos\vartheta + h_e)$$

$$\tilde{L}_{-0}^+ (h_e) = -\sqrt{1-z} \tilde{L}_{0+}^+ (-h_e) = -4 \frac{\sqrt{1-z}}{z} (-\cos\vartheta + h_e) e^{-2i\chi}$$

and those of the hadron tensor,

$$\begin{aligned} \tilde{H}_{--}^+(h_q) &= (1-z) \tilde{H}_{++}^+(-h_q) = \sqrt{2} x_{\perp} (1-z) \left\{ \frac{1}{z} \left[\frac{1-x_q}{1-x_{\bar{q}}} + \frac{1-x_{\bar{q}}}{1-x_q} \right] \right. \\ &\quad \left. + h_q \left[\frac{1}{1-x_q} - \frac{1}{1-x_{\bar{q}}} \right] \right\} \\ \tilde{H}_{00}^+ &= 4 \sqrt{2} \frac{x_{\perp}}{z} \sqrt{1-z} \\ \tilde{H}_{-+}^+ &= (1-z) \tilde{H}_{+-}^+ = 2 \sqrt{2} x_{\perp} \frac{1-z}{z} \\ \tilde{H}_{0-}^+(h_q) &= -\sqrt{1-z} \tilde{H}_{-0}^+(h_q) = -\sqrt{1-z} \tilde{H}_{+0}^+(-h_q) = -\tilde{H}_{0+}^+(-h_q) \\ &= -4 \frac{1-z}{z} \left[\frac{x_{\bar{q}} - x_q}{z} - h_q \right] \end{aligned}$$

\mathcal{CP} invariance of the theory relates the negative real γ helicity to the positive helicity matrix elements,

$$\begin{aligned} \tilde{L}_{mn}^-(\chi; h_e) &= (-)^{m+n+1} \tilde{L}_{-m-n}^+(-\chi; -h_e) \\ \tilde{H}_{mn}^-(h_q) &= (-)^{m+n+1} \tilde{H}_{-m-n}^+(-h_q) \quad , \end{aligned}$$

completing the set of spin density matrices in the interference term of the γ cross section.

Appendix B

QCD Corrections to Direct Photon Cross Sections

In this second appendix we list the first order QCD corrections to the Born terms introduced in eqs. (21) to (23) of Section 2.

$$\begin{aligned}
 s_L^q = & \frac{x_\perp^2}{(1-x_q)(1-x_{\bar{q}})} \left\{ 2 \ln \varepsilon \left[\ln \left(\frac{1-\cos\delta}{2} \right) - \ln \left(\frac{1-\cos\vartheta_{q\bar{q}}}{2} \right) \right] \right. \\
 & - \ln \left(\frac{1-\cos\delta}{2} \right) \left(-\frac{3}{2} + \frac{\varepsilon}{x_q} + \frac{\varepsilon}{x_{\bar{q}}} + \ln x_q + \ln x_{\bar{q}} \right) - \frac{5}{2} + \frac{1}{3} \pi^2 \\
 & + \mathcal{L}_2 \left(\frac{1-\cos\vartheta_{q\bar{q}}}{2} \right) - \mathcal{L}_2(1-z) - \frac{1}{2} \mathcal{L}_2(1-x_q) - \frac{1}{2} \mathcal{L}_2(1-x_{\bar{q}}) \\
 & - \frac{1}{2} \ln^2 \left(\frac{1-\cos\vartheta_{q\bar{q}}}{2} \right) - \ln^2 x_q - \ln^2 x_{\bar{q}} + \frac{3}{2} (\ln x_q + \ln x_{\bar{q}}) \\
 & - \frac{1}{2} \left(\ln x_q \ln(1-x_q) + \ln x_{\bar{q}} \ln(1-x_{\bar{q}}) \right) - \ln(1-z) \left(1 - \frac{1}{2} \ln \frac{x_\perp^2}{4} \right) \\
 & - \ln(1-x_q) \frac{1}{4} \frac{1}{1-z} (1-x_{\bar{q}}) \left(\frac{1+x_q}{x_q} \right) \left(1 - \frac{1-x_{\bar{q}}}{x_q} \right) \\
 & - \ln(1-x_{\bar{q}}) \frac{1}{4} \frac{1}{1-z} (1-x_q) \left(\frac{1+x_{\bar{q}}}{x_{\bar{q}}} \right) \left(1 - \frac{1-x_q}{x_{\bar{q}}} \right) \\
 & \left. - \frac{1}{4} \frac{1}{1-z} \left(z - \frac{(1-x_{\bar{q}})^2}{x_q} - \frac{(1-x_q)^2}{x_{\bar{q}}} \right) \right\}
 \end{aligned}$$

\mathcal{L}_2 denotes the dilogarithm,

$$\mathcal{L}_2(x) = - \int_0^x dz \frac{\log(1-z)}{z}$$

with

$$\mathcal{L}_2(1) = \frac{\pi^2}{6}$$

$$\begin{aligned}
s_T^q + s_L^q = & B_V(x_q, x_{\bar{q}}) \left\{ 2 \ln \epsilon \left[\ln \left(\frac{1 - \cos \delta}{2} \right) - \ln \left(\frac{1 - \cos \vartheta_{q\bar{q}}}{2} \right) \right] \right. \\
& - \ln \left(\frac{1 - \cos \delta}{2} \right) \left(-\frac{3}{2} + \frac{\epsilon}{x_q} + \frac{\epsilon}{x_{\bar{q}}} + \ln x_q + \ln x_{\bar{q}} \right) - \frac{5}{2} + \frac{1}{3} \pi^2 \\
& + \mathcal{L}_2 \left(\frac{1 - \cos \vartheta_{q\bar{q}}}{2} \right) - \mathcal{L}_2(1-z) - \left(\mathcal{L}_2(1-z) - \frac{\pi^2}{6} \right) - \mathcal{L}_2(1-x_q) \\
& - \mathcal{L}_2(1-x_{\bar{q}}) - \frac{1}{2} \ln^2 \left(\frac{1 - \cos \vartheta_{q\bar{q}}}{2} \right) - \ln^2 x_q - \ln^2 x_{\bar{q}} \\
& + \frac{3}{2} (\ln x_q + \ln x_{\bar{q}}) - \ln x_q \ln(1-x_q) - \ln x_{\bar{q}} \ln(1-x_{\bar{q}}) \\
& \left. - \ln(1-z) \left[2 \ln z - \ln(1-x_q) - \ln(1-x_{\bar{q}}) - \frac{1}{2} \ln(1-z) \right] \right\} \\
& + B_S(x_q, x_{\bar{q}}) \left[\frac{1}{2} + \mathcal{L}_2(1-z) - \frac{\pi^2}{6} + \ln z \ln(1-z) \right] \\
& + F_1(x_q, x_{\bar{q}}) \left[\ln x_q \ln(1-x_q) + \mathcal{L}_2(1-x_q) - \ln(1-z) \ln(1-x_q) \right] \\
& + F_1(x_{\bar{q}}, x_q) \left[\ln x_{\bar{q}} \ln(1-x_{\bar{q}}) + \mathcal{L}_2(1-x_{\bar{q}}) - \ln(1-z) \ln(1-x_{\bar{q}}) \right] \\
& + F_2(x_q, x_{\bar{q}}) \left[\mathcal{L}_2(1-z) - \frac{\pi^2}{6} + \ln z \ln(1-z) \right] + F_3(x_q, x_{\bar{q}}) \ln(1-x_q) \\
& + F_3(x_{\bar{q}}, x_q) \ln(1-x_{\bar{q}}) + 2 \ln(1-z) \left(1 - \frac{1}{z} \right) + F_4(x_q, x_{\bar{q}})
\end{aligned}$$

The B and F functions are abbreviations of

$$B_V(x_q, x_{\bar{q}}) = \frac{x_q^2 + x_{\bar{q}}^2}{(1-x_q)(1-x_{\bar{q}})}$$

$$B_S(x_q, x_{\bar{q}}) = \frac{z^2}{(1-x_q)(1-x_{\bar{q}})}$$

$$F_1(x_q, x_{\bar{q}}) = \left(-2 + \frac{x_q}{1-x_q} + \frac{1}{1-x_{\bar{q}}} \right)$$

$$F_2(x_q, x_{\bar{q}}) = \left(-6 + \frac{2x_q}{1-x_{\bar{q}}} + \frac{2x_{\bar{q}}}{1-x_q} \right)$$

$$F_3(x_q, x_{\bar{q}}) = \left(-1 + \frac{1}{2} \frac{1}{x_q^2} (1-x_q) + \frac{1}{2} \frac{1}{x_{\bar{q}}^2} (1-x_{\bar{q}}) - \frac{3}{2} \frac{x_{\bar{q}}}{x_q} \right)$$

$$F_4(x_q, x_{\bar{q}}) = -1 + \frac{1}{2} \frac{1}{x_q} (1-x_q) + \frac{1}{2} \frac{1}{x_{\bar{q}}} (1-x_{\bar{q}}) + \frac{1}{2} \left(\frac{x_q}{1-x_{\bar{q}}} + \frac{x_{\bar{q}}}{1-x_q} \right) - \frac{2}{z}$$

For the radiation off the lepton line we get

$$\begin{aligned} s_{L/T}^e = B_{L/T}^e & \left\{ 2 \ln \varepsilon \left(\ln \left(\frac{1-\cos\delta}{2} \right) - \ln \left(\frac{1-\cos\vartheta}{2} \right) \right) \right. \\ & - \ln \left(\frac{1-\cos\delta}{2} \right) \left(-\frac{3}{2} + \frac{\varepsilon}{x_q} + \frac{\varepsilon}{x_{\bar{q}}} + \ln x_q + \ln x_{\bar{q}} \right) - \frac{5}{2} + \frac{1}{3} \pi^2 \\ & + \left(\mathcal{L}_2 \left(\frac{1-\cos\vartheta}{2} \right) - \frac{\pi^2}{6} \right) - \frac{1}{2} \ln^2 \left(\frac{1-\cos\vartheta}{2} \right) - \ln^2 x_q - \ln^2 x_{\bar{q}} \\ & \left. + \frac{3}{2} \left(\ln x_q + \ln x_{\bar{q}} \right) + \frac{1}{2} \ln^2(1-z) - \frac{3}{2} \ln(1-z) \right\} \end{aligned}$$

where

$$B_L^e = \frac{x_1^2}{z^2(1-z) \sin^2\vartheta}$$

$$B_T^e = \frac{x_q^2 + x_{\bar{q}}^2 - x_1^2}{z^2(1-z) \sin^2\vartheta}$$

The correction to the interference term is given by

$$\begin{aligned}
 s_i = & -4 \frac{2-z}{z^2} \left\{ 2 \ln \varepsilon \left(\ln \left(\frac{1-\cos\delta}{2} \right) - \ln \left(\frac{1-\cos\vartheta_{q\bar{q}}}{2} \right) \right) \right. \\
 & - \ln \left(\frac{1+\cos\delta}{2} \right) \left(-\frac{3}{2} + \frac{\varepsilon}{x_q} + \frac{\varepsilon}{x_{\bar{q}}} + \ln x_q + \ln x_{\bar{q}} \right) - \frac{5}{2} + \frac{1}{3} \pi^2 \\
 & + \mathcal{L}_2 \left(\frac{1-\cos\vartheta_{q\bar{q}}}{2} \right) - \mathcal{L}_2(1-z) + \frac{1}{2} \left(\mathcal{L}_2(1-z) - \frac{\pi^2}{6} \right) \\
 & - \frac{1}{2} \mathcal{L}_2(1-x_q) \frac{x_q}{x_q+x_{\bar{q}}} - \frac{1}{2} \mathcal{L}_2(1-x_{\bar{q}}) \frac{x_{\bar{q}}}{x_q+x_{\bar{q}}} - \frac{1}{2} \ln^2 \left(\frac{1-\cos\vartheta_{q\bar{q}}}{2} \right) \\
 & - \ln^2 x_q - \ln^2 x_{\bar{q}} + \frac{3}{2} (\ln x_q + \ln x_{\bar{q}}) - \frac{1}{2} \left[\ln x_q \ln(1-x_{\bar{q}}) \frac{x_q}{x_q+x_{\bar{q}}} \right. \\
 & \left. + \ln x_{\bar{q}} \ln(1-x_q) \frac{x_{\bar{q}}}{x_q+x_{\bar{q}}} \right] \\
 & - \ln(1-z) \left[+ \frac{1}{2} \ln z - \frac{1}{2} \ln(1-z) - \frac{1}{2} \ln(1-x_{\bar{q}}) \frac{x_{\bar{q}}}{x_q+x_{\bar{q}}} \right. \\
 & \left. - \frac{1}{2} \ln(1-x_q) \frac{x_q}{x_q+x_{\bar{q}}} - \frac{1}{2} \frac{1}{x_q+x_{\bar{q}}} + \frac{5}{4} \right] \\
 & + \frac{1}{4} \ln(1-x_q) \left[\frac{1}{x_q} (1+x_q) \left(\frac{1}{x_q+x_{\bar{q}}} - z \right) + \frac{1-x_{\bar{q}}}{x_q+x_{\bar{q}}} - 1 \right] \\
 & + \frac{1}{4} \ln(1-x_{\bar{q}}) \left[\frac{1}{x_{\bar{q}}} (1+x_{\bar{q}}) \left(\frac{1}{x_q+x_{\bar{q}}} - z \right) + \frac{1-x_q}{x_q+x_{\bar{q}}} - 1 \right] \\
 & \left. - \frac{1}{4} \frac{(x_q+x_{\bar{q}})}{x_q x_{\bar{q}}} z + \frac{1}{2} \left(\frac{1}{x_q+x_{\bar{q}}} - \frac{1}{2} \right) + \frac{1}{4} \left(\frac{1}{x_q x_{\bar{q}}} - 1 \right) \right\}
 \end{aligned}$$

Note that the leading contributions for $\varepsilon, \delta \rightarrow 0$ are universal,

$$\begin{aligned}
 d\sigma_{\text{BORN}} \rightarrow d\sigma = & d\sigma_{\text{BORN}} \left\{ 1 - \frac{4\alpha_s}{3\pi} \left[2 \log \varepsilon \left(\log \frac{\delta^2}{4} - \log \left(\frac{1-\cos\vartheta_{q\bar{q}}}{2} \right) \right) \right. \right. \\
 & \left. \left. - \log \frac{\delta^2}{4} \left(-\frac{3}{2} + \log x_q + \log x_{\bar{q}} \right) \right] \right\}
 \end{aligned}$$

For $z \rightarrow 0$ we rediscover the Serman-Weinberg correction factor, as expected on general grounds,

$$d\sigma_{\text{BORN}} \rightarrow d\sigma = d\sigma_{\text{BORN}} \left\{ 1 - \frac{4\alpha_s}{3\pi} \left[2 \log \varepsilon \log \frac{\delta^2}{4} - \log \frac{\delta^2}{4} \left(-\frac{3}{2} + 2\varepsilon \right) - \frac{5}{2} + \frac{1}{3} \pi^2 + \mathcal{O}(z) \right] \right\}$$

Table 1

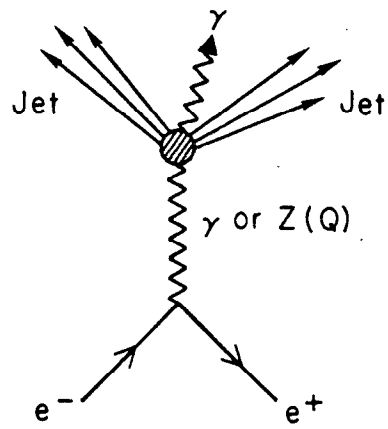
Combinations of coupling constants which can be measured on the Z under various experimental conditions of beam polarization and quark-charge identification.

	el. quark charge not identified	el. quark charge identified
no beam polarization	$(v_e^2 + a_e^2) \cdot e_q^2 (v_q^2 + a_q^2)$	$v_e a_e \cdot e_q^2 v_q a_q$
longitudinal beam polarization	$v_e a_e \cdot e_q^2 (v_q^2 + a_q^2)$	$(v_e^2 + a_e^2) \cdot e_q^2 v_q a_q$

FIGURE CAPTIONS

- Fig. 1 $e^+e^- \rightarrow \gamma + \text{two jets}$. The photon is emitted from the final (hadronic) state.
- Fig. 2 The three regimes for photon radiation off the final quarks:
a) large angle emission; b) small angle emission of a hard photon; c) emission of photons at limited transverse momentum $p_{\perp} = \mathcal{O}(\Lambda)$.
- Fig. 3 Kinematics for $e^+e^- \rightarrow q\bar{q}\gamma$.
- Fig. 4 Representative Feynman graphs for γ radiation off the quark (a) and lepton lines (b) up to order α_s .
- Fig. 5a The total cross section for direct photon production normalized to the $e^+e^- \rightarrow q\bar{q}$ cross section.
- Fig. 5b The relative contributions $\sigma^j(q\bar{q}\gamma) / \sum_k \sigma^k(q\bar{q}\gamma)$ for radiation off quarks, leptons and the interference term.
- Fig. 6 The γ spectrum for $Q = 30$ GeV and on the Z. For comparison we also show the typical hadronic shape of the spectrum from quark fragmentation.
- Fig. 7 The dependence of the various contributions to the direct γ cross section on the angle between quark and photon.
- Fig. 8 The charge asymmetry as a function of the angle between quark and photon.
- Fig. 9 The Sterman-Weinberg jet definition for direct γ production.
- Fig. 10 Born term and QCD corrections for the total cross section, and the radiation off quarks, leptons and the interference term (cf. eqs. (21-23)).

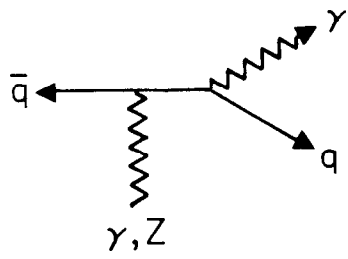
- Fig. 11 Ratios of cross sections for Born terms and QCD corrections as a function of the photon energy. " $(\sigma_L/\sigma_T)_e$ " is unaffected by QCD corrections of order α_s (cf. Appendix B).
- Fig. 12 The cross section as a function of the angle between photon and quark, Born term and QCD corrections.
- Fig. 13 Transverse and longitudinal fragmentation functions. For \bar{F}_T we show the Born term, the leading log contribution LL (both with $\log(1-z)Q^2/\Lambda^2$) and the subleading log. For comparison the Born term and leading log are also shown for $\log Q^2/\Lambda^2$ (dotted lines).
- Fig. 14 Qualitative features of the photon spectrum at present energies in two extreme scenarios. a) Perturbative parton evolution gets superseded by nonperturbative effects at invariant parton masses of the order of 5 GeV. b) Perturbative parton evolution continues down to invariant masses of the order the ρ mass.



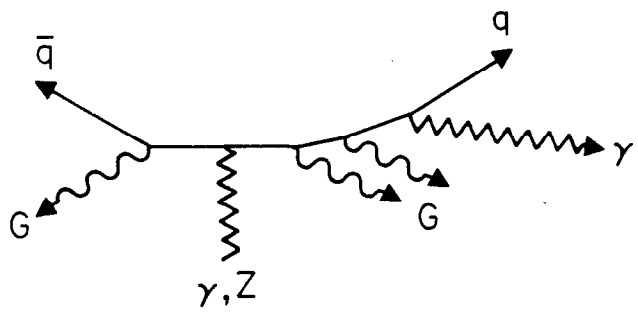
4-82

4297A1

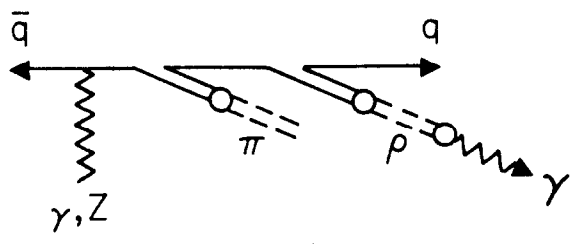
Fig. 1



(a)



(b)

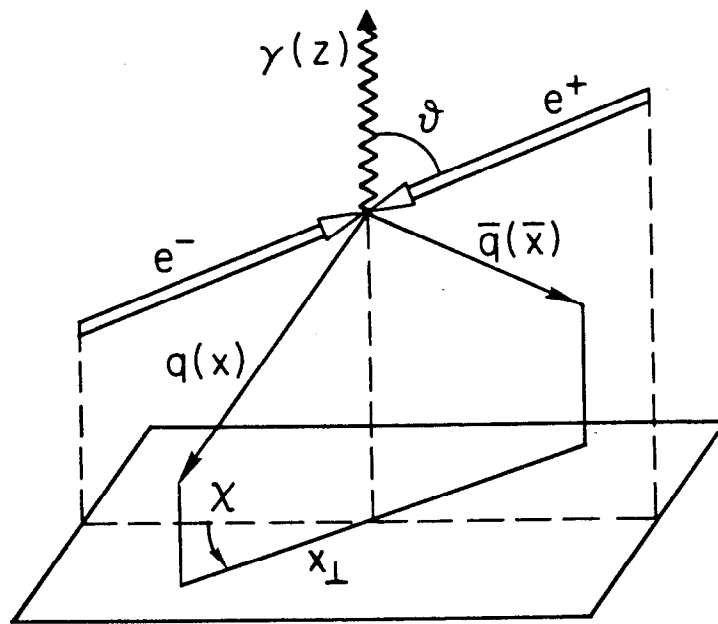


(c)

4-82

4297A2

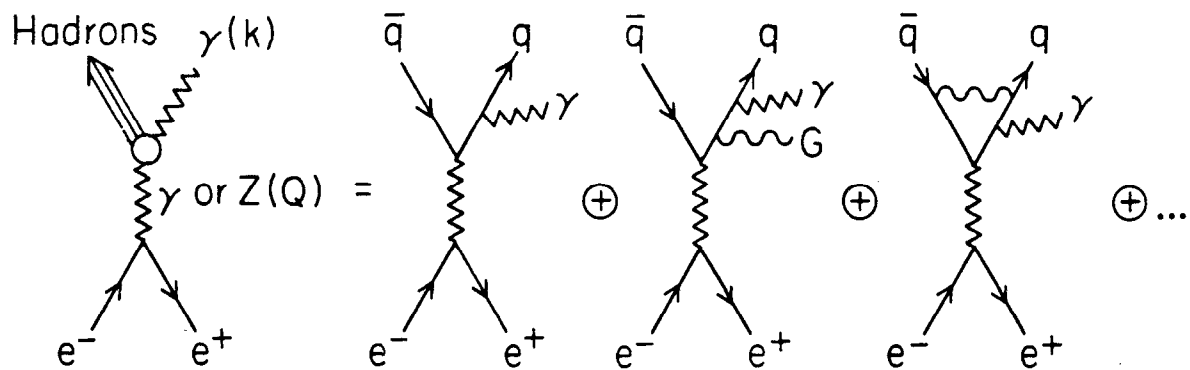
Fig. 2



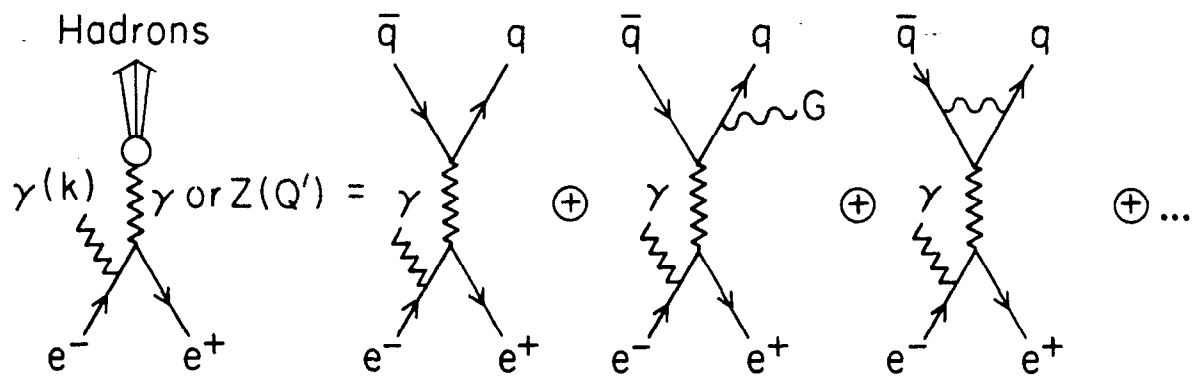
4-82

4297A3

Fig. 3



(a)



(b)

Fig. 4

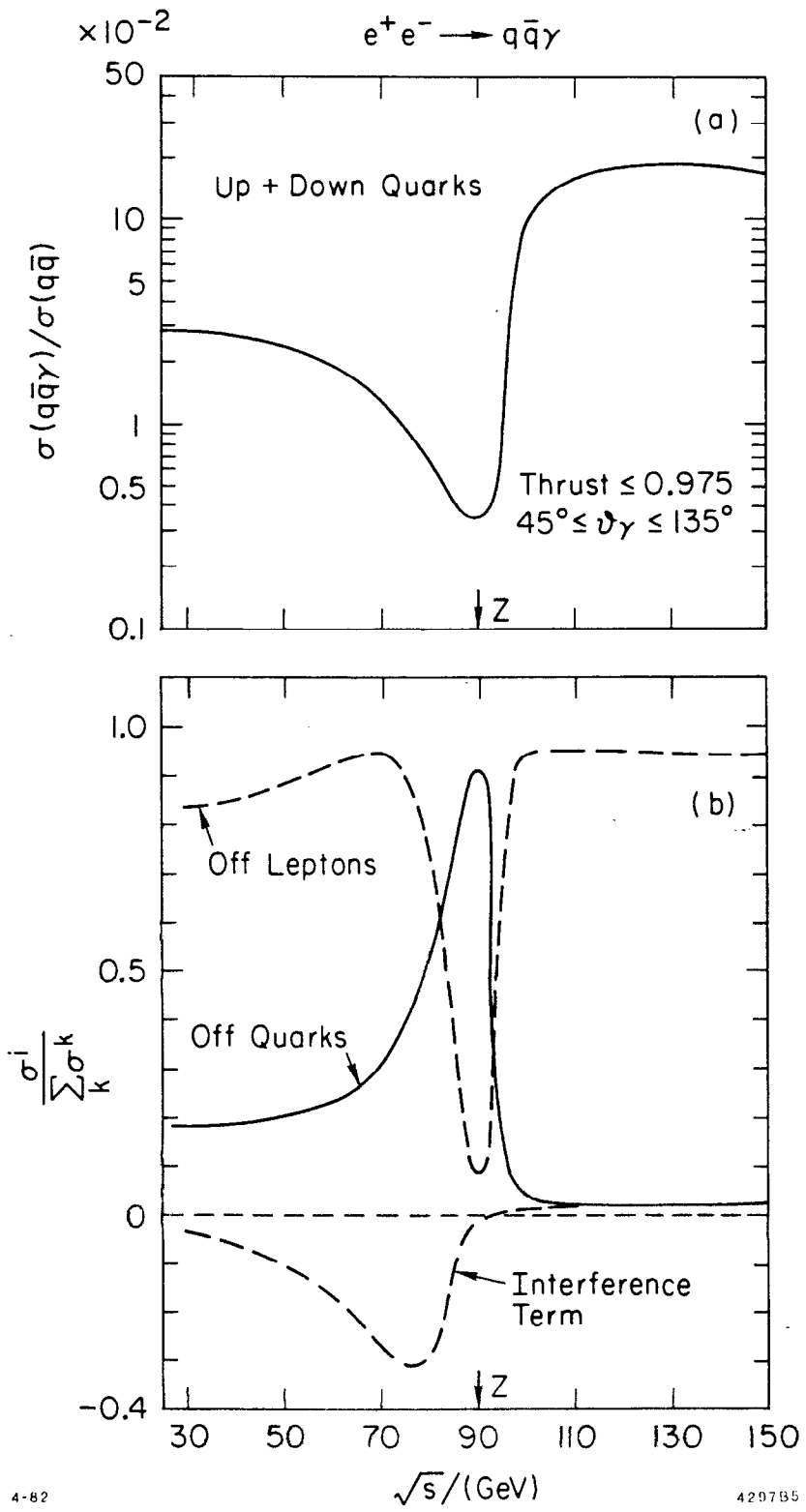


Fig. 5

$e^+e^- \rightarrow \gamma + 2 \text{ Jets}$

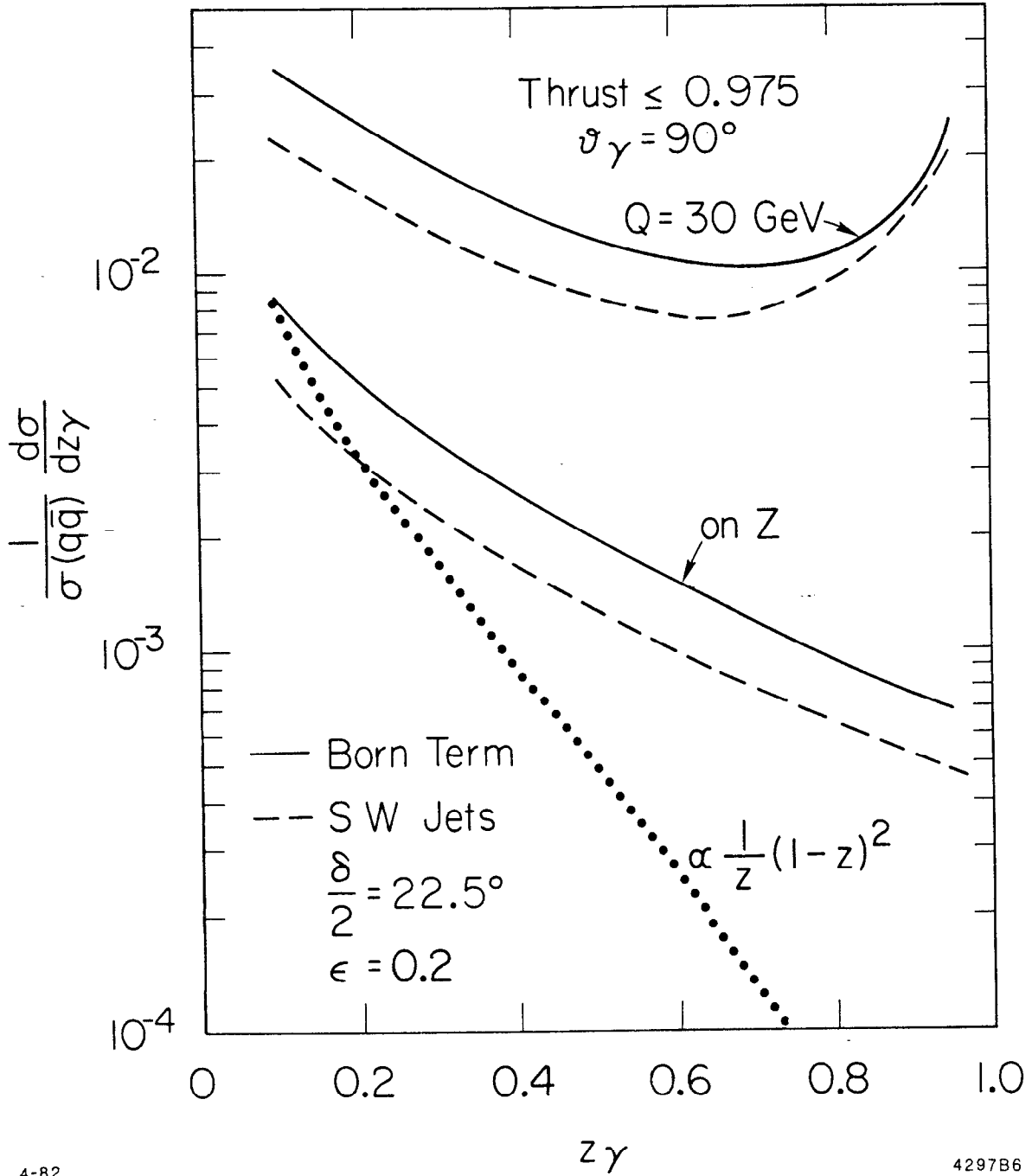


Fig. 6

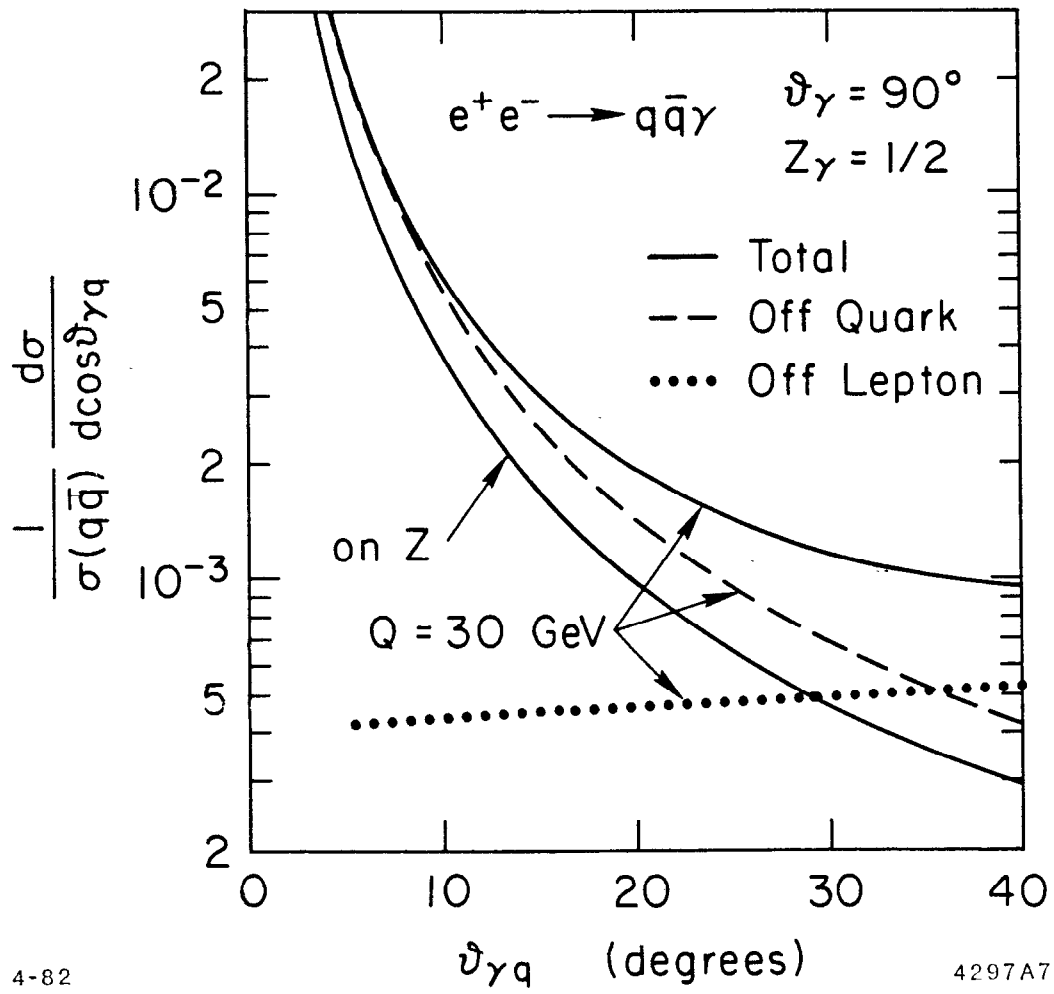


Fig. 7

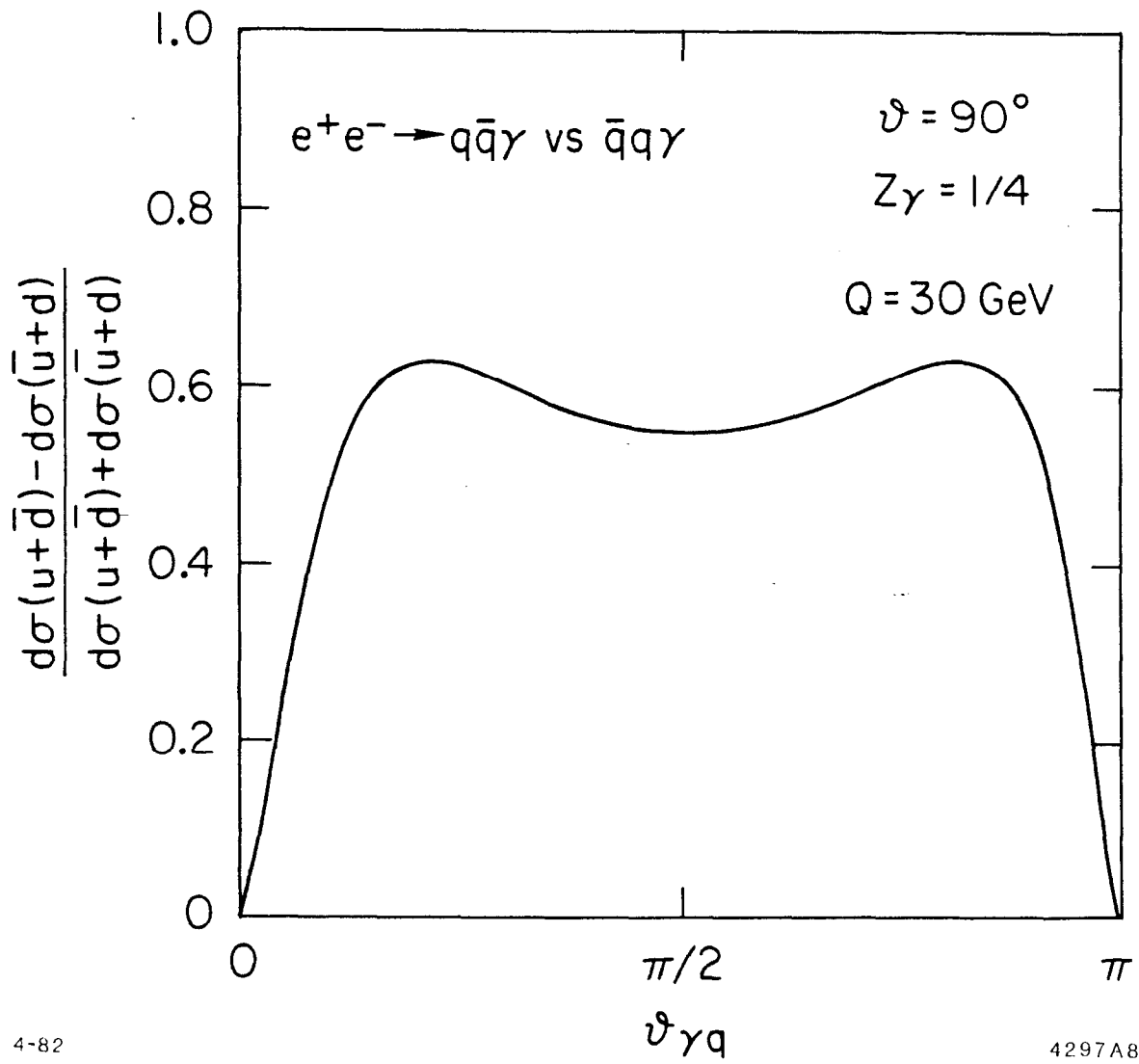


Fig. 8

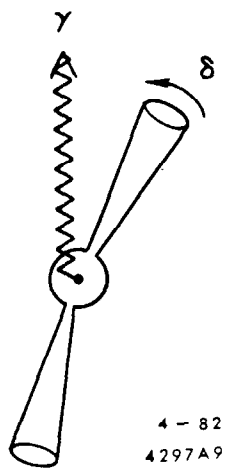


Fig. 9

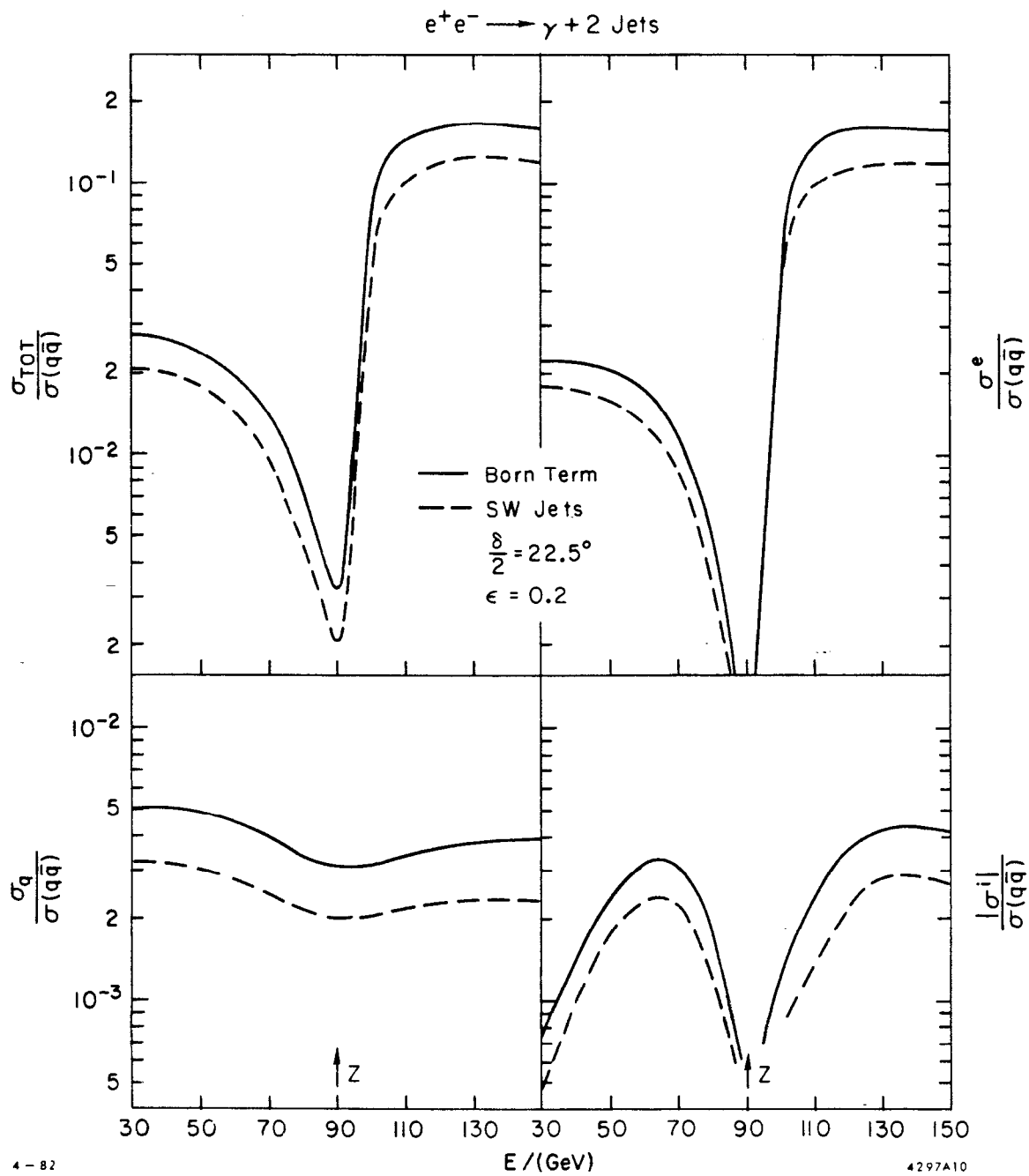


Fig. 10

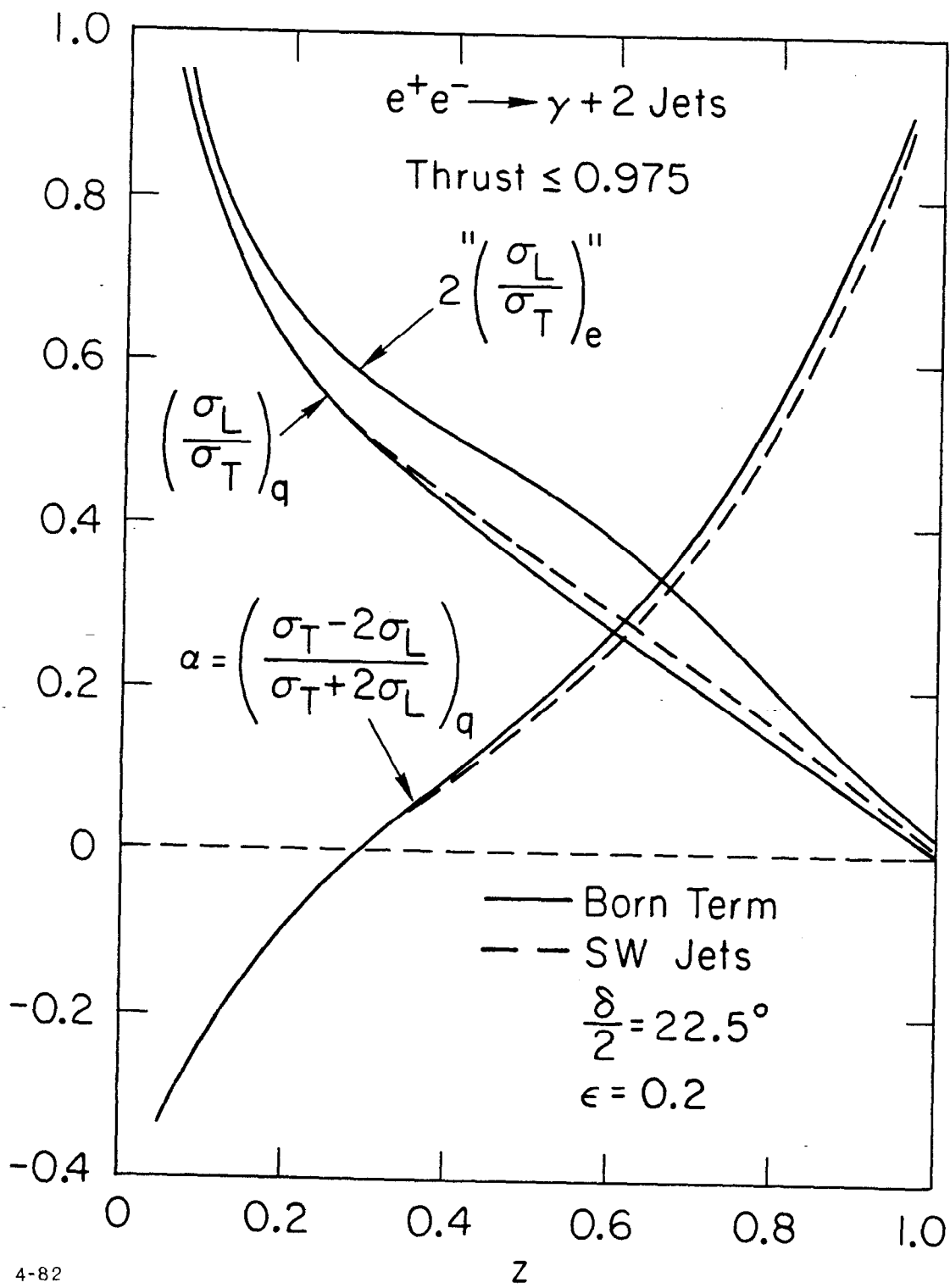


Fig 11

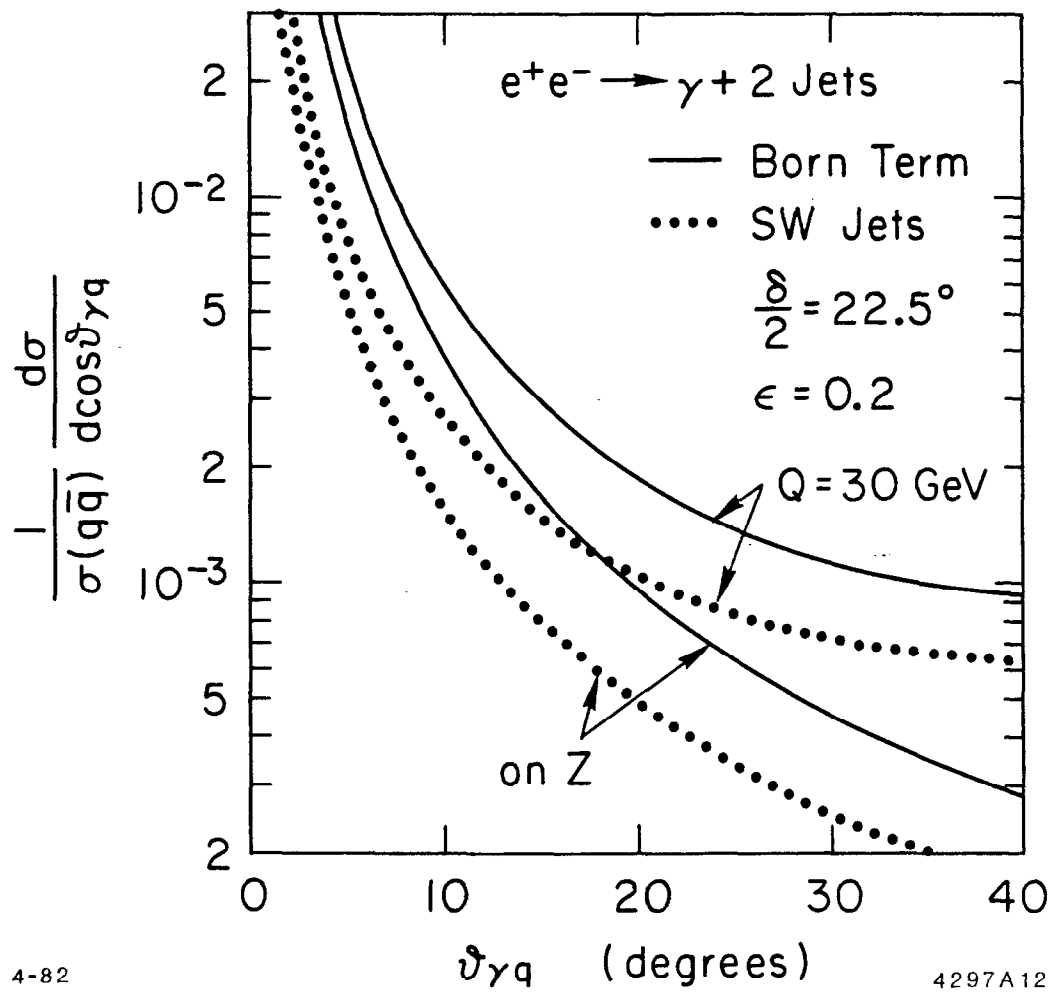


Fig. 12

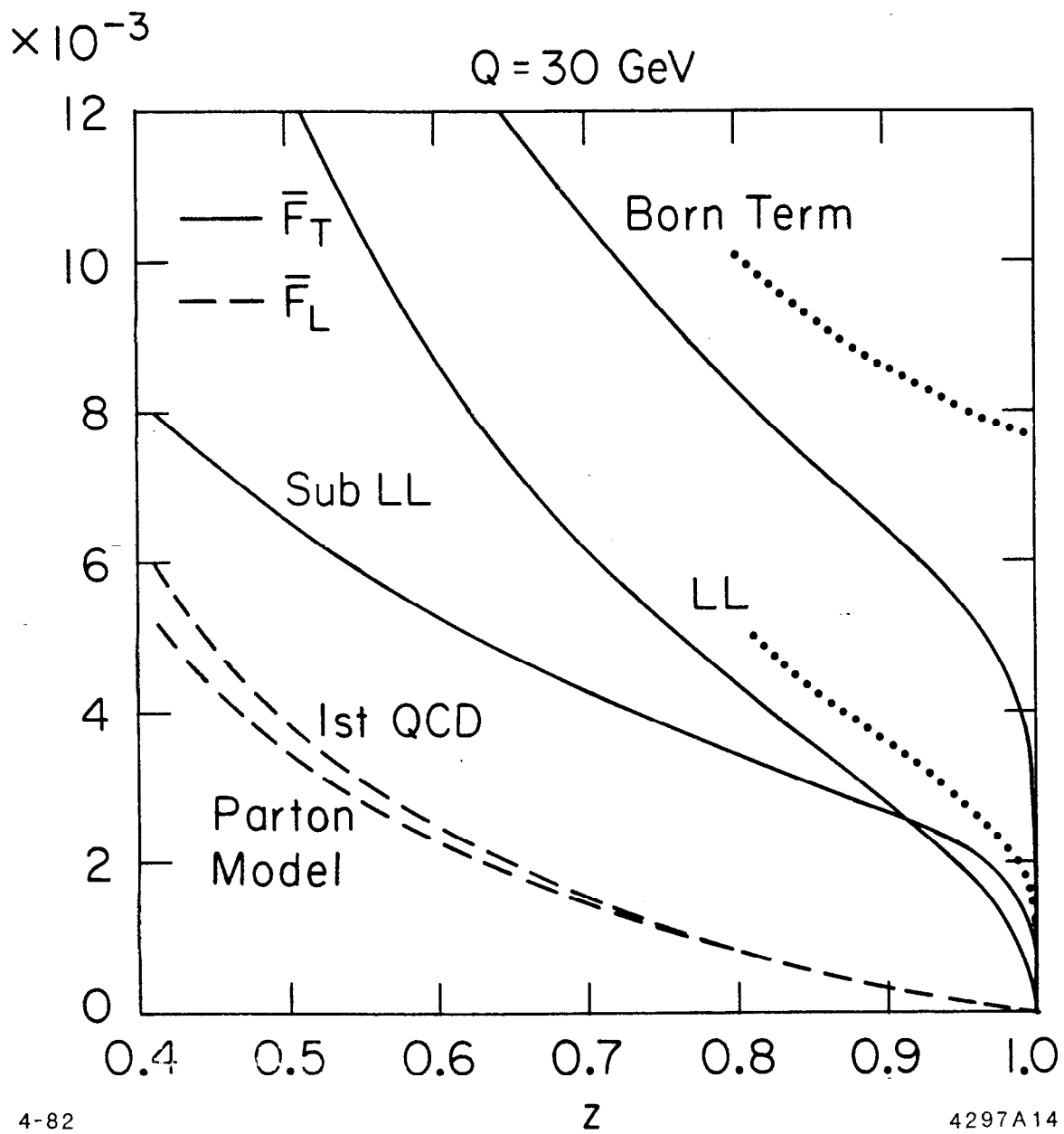


Fig. 13

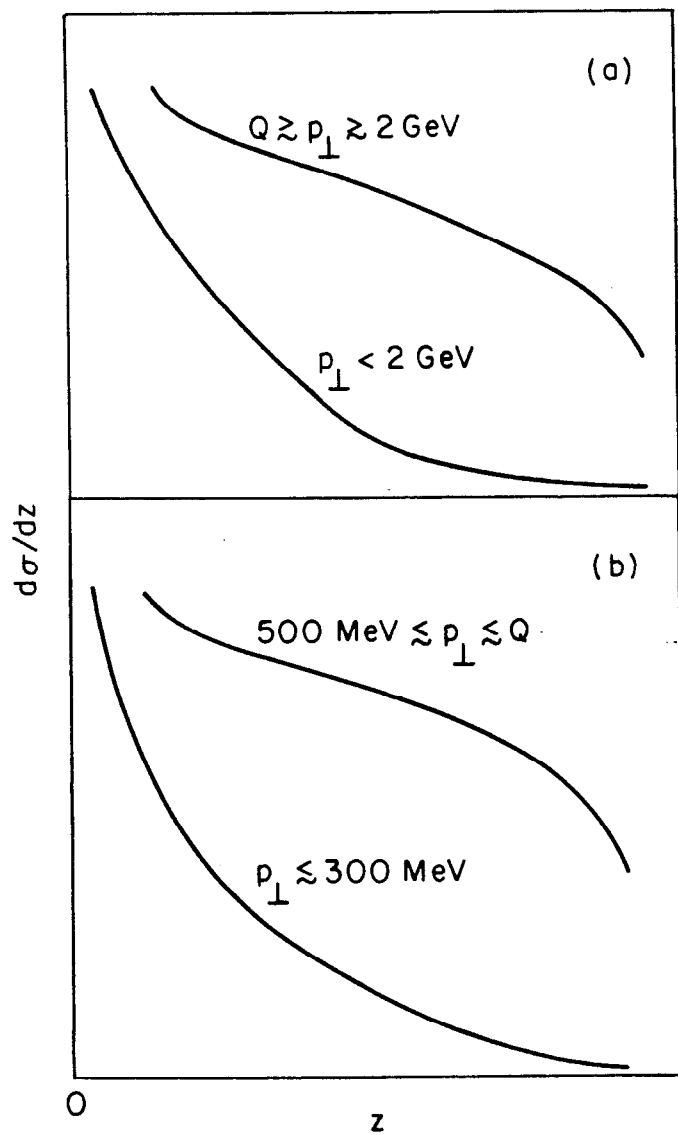


Fig. 14